Photoinduced transient Faraday rotation in NiO

Takuya Satoh,[1,*] Sung-Jin Cho,[1] Tsutomu Shimura,[1] Kazuo Kuroda,[1] Hiroaki Ueda,[2] Yutaka Ueda,[2] and Manfred Fiebig[3]

[1]*Institute of Industrial Science, University of Tokyo, Tokyo 153-8505, Japan*
[2]*Institute for Solid State Physics, University of Tokyo, Kashiwa, Chiba 277-8581, Japan*
[3]*HISKP, Universität Bonn, Nussallee 14-16, 53115 Bonn, Germany*
[*]*Corresponding author: tsatoh@iis.u-tokyo.ac.jp*

Received April 7, 2010; accepted April 29, 2010;
posted May 13, 2010 (Doc. ID 126651); published June 18, 2010

A non-thermal ultrafast magneto-optical response of antiferromagnetic NiO to irradiation with an intense optical pulse was observed. With temporally overlapping pump and probe pulses, the circularly polarized pump pulse induced rotation of the linear polarization of the probe pulse along with two-photon absorption and cross-phase modulation. The sign of the rotation of the linear polarization reversed with the reversal of the pump helicity. This non-resonant phenomenon is described as a third-order nonlinear optical effect and is ascribed to an inverse Faraday effect: photoinduced magnetization. © 2010 Optical Society of America

OCIS codes: 190.7110, 160.3820.

1. INTRODUCTION

The ultrafast magneto-optical response of materials pumped by circularly polarized light pulses has been studied extensively in recent years. One effect is the inverse Faraday effect (IFE), where the magnetization is generated along the wave vector of the circularly polarized light. This magnetization leads to Faraday rotation of the probe light polarization. The IFE arises from an optically induced Stark effect that lifts the degeneracy of the electronic ground state [1]. Phenomenologically, the IFE is described as a third-order nonlinear optical effect [2]. In a pump-probe geometry using femtosecond pulses, the magnetization generated by the IFE occurs at $t=0$ when the pump and probe pulses temporally overlap [3–8]. In the same temporal region, however, other third-order nonlinear optical effects, such as two-photon absorption, have been observed [9]. Separation of the IFE from the other effects within a single experiment has not been carried out yet.

It has been proposed that ultrafast manipulation of the antiferromagnetic (AFM) order parameter may be employed for ultrafast control of the magnetization of an adjacent ferromagnet via the exchange-bias effect [10]. NiO is one of the most promising exchange-bias antiferromagnets because of its simple structure and room-temperature antiferromagnetism. In addition, ultrafast magnetization switching in AFM NiO is possible via spin-orbit interaction in a spin-mixed excited state [11]. Inspired by this, we have investigated the time-resolved magneto-optical response of NiO excited by a circularly polarized pulse. In this paper, we report on the estimation of the nonlinear optical susceptibility of the IFE in NiO in a pump-probe experiment. The non-thermally photoinduced magnetization was accompanied by two-photon absorption and cross-phase modulation, which modulated the polarization and the intensity of a probe pulse transmitted through the sample. The modulation was restricted to the duration of the pump pulse and can therefore serve as the basis for magnetization control in NiO at sub-picosecond duty cycles.

The Faraday effect is a circular birefringence arising from the imaginary part of the antisymmetric components in the dielectric tensor caused by a magnetization [12]. In the IFE, a circularly polarized pump pulse induces a magnetization along the beam direction, resulting in Faraday rotation of the probe pulse. In the pump-probe geometry, the polarization P is given by [2]

$$P_j(\omega_p) = \epsilon_0 \sum_k \chi^{(1)}_{jk}(\omega_p) E_k(\omega_p) + \epsilon_0 \sum_{klm} \chi^{(3)}_{jklm}(\omega_p, \omega_e, -\omega_e) E_k(\omega_p) E_l(\omega_e) E^*_m(\omega_e), \tag{1}$$

where subscripts e and p denote the pump and probe, respectively; ϵ_0 is the permittivity of vacuum; $\chi^{(n)}$ is the nonlinear optical susceptibility of order n; and E and E^* are the electric field and its conjugate, respectively. The pump-induced dielectric tensor $\Delta\epsilon$ is

$$\Delta\epsilon_{jk}(\omega_p, \omega_e) = \sum_{lm} \chi^{(3)}_{jklm} E_l(\omega_e) E^*_m(\omega_e). \tag{2}$$

For a σ_+ polarized pump pulse, the electric field propagating along the z direction is given by

$$\mathbf{E}(\omega_e) = \frac{E_0}{\sqrt{2}} \begin{pmatrix} 1 \\ i \\ 0 \end{pmatrix} \exp[i(\omega_e t - kz)]. \tag{3}$$

An isotropic medium reveals $\chi^{(3)}_{xyxx} = \chi^{(3)}_{xyyy} = \chi^{(3)}_{yxxx} = \chi^{(3)}_{yxyy} = 0$, $\chi^{(3)}_{xyxy} = \chi^{(3)}_{yxyx}$, $\chi^{(3)}_{xyyx} = \chi^{(3)}_{yxxy}$ [1] so that the antisymmetric components of the dielectric tensor $\Delta\epsilon_{jk}$ are obtained as [2]

$$\Delta\epsilon_{xy} = -\Delta\epsilon_{yx} = \frac{1}{2}(\chi^{(3)}_{xyxy} - \chi^{(3)}_{xyyx})(\mathbf{E}\times\mathbf{E}^*)_z$$

$$= i\frac{E_0^2}{2}(-\chi^{(3)}_{xyxy} + \chi^{(3)}_{xyyx}). \quad (4)$$

The real part of $(-\chi^{(3)}_{xyxy}+\chi^{(3)}_{xyyx})$ gives rise to the Faraday rotation of the probe beam. Further, the rotation angle is proportional to the pump pulse intensity. For a σ_- polarized pump pulse, the sign of $\Delta\epsilon_{xy}$ is reversed. Thus, the Faraday rotation angle is reversed with the reversal of the pump helicity.

2. EXPERIMENT

A NiO crystal possesses a NaCl-type cubic structure in the paramagnetic state. Below the Néel temperature (T_N=523 K), NiO sets in AFM order with antiparallel stacking of {111} ferromagnetic sheets. The exchange coupling of Ni^{2+} ions leads to a contraction of the cubic unit cell along the ⟨111⟩ axes, giving rise to four types of twin (T) domains (T_0–T_3). The T domains are visualized as shown below (Fig. 1) with the magnetic birefringence between the {111} plane and the ⟨111⟩ direction [13].

A NiO single crystal was grown by a floating zone method. (111)-oriented platelets with a thickness of ≃100 μm were prepared. The sample was annealed in an argon-oxygen mixture with small oxygen partial pressure at 1400°C to obtain T domains of 0.1–1 mm [14].

For the pump-probe measurement we selected the T_0 domain of ≈500 μm whose local [111] direction is oriented perpendicular to the surface of the sample. Therefore, the laser light propagates along the optical axis of the T_0 domain and does not experience linear birefringence. This ensures that the circularly polarized pump pulse retains its polarization throughout the sample so that other third-order nonlinear optical effects, such as the optical Kerr effect, are negligible. Further, the detection of Faraday rotation is greatly simplified by the absence of linear birefringence [15]. In order to select a T_0 domain, a cross-Nicol arrangement was employed as schematically illustrated in Fig. 1(a) [13]. Figures 1(b)–1(d) reveal the distribution of T domains of a NiO sample at room temperature with polarizer angles of 0°, 30°, and 60°, respectively. By rotating the polarizer and analyzer with the cross-Nicol configuration, the four types of T domains were distinguished. Whereas the T_1–T_3 domains showed birefringence with a relative shift of 30° in the angular dependence of different domains, the T_0 domains were always black in the cross-Nicol images because of their optical isotropy [Fig. 1(e)].

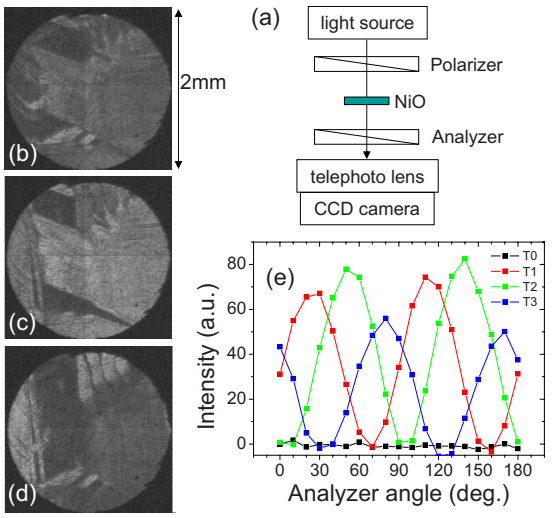

Fig. 1. (Color online) (a) Cross-Nicol transmission imaging setup. (b),(c),(d) Cross-Nicol transmission image of a NiO (111) crystal. Polarizer angles were 0°, 30°, and 60°, respectively. (e) Dependence of transmission of light through T_0–T_3 domains on the angle of the analyzer in the cross-Nicol configuration.

The time-resolved Faraday rotation and transmission were measured at room temperature with a pump-probe setup. The setup is based on an optical parametric amplifier pumped by a Ti:sapphire laser with a wavelength of 792 nm, a pulse width of 120 fs, and a repetition rate of 1 kHz. The sample was excited by circularly polarized pump pulses with wavelengths of λ_e=1280 and 792 nm at a repetition rate of 500 Hz. We measured the Faraday rotation and transmission of the linearly polarized probe beam at λ_p=840 nm because the maximum transmission of the NiO samples was at this wavelength in the 300–1400 nm range investigated here [16]. To generate the probe beam, a white-light continuum (WLC) obtained by self-phase modulation of the Ti:sapphire laser pulse at 792 nm during propagation through a sapphire plate was employed. A bandpass filter was used to select light at 840 nm from the WLC. A wave plate and a polarizer were used to set the polarization of the incoming beams. The intensity ratio of the pump to probe light was $>10^3$ so that the influence of the probe light on the medium was negligible. The diameters of the pump and probe beams were 100 and 40 μm, respectively. The probe light fell on the sample at normal incidence, whereas the pump light was incident at an angle of 7°. The transmitted probe light was detected after suppressing residual pump light with a bandpass or a color-glass filter. The probe beam was divided into two orthogonally polarized components by a Wollaston prism, and each beam was detected with a Si photodiode. Each signal was sent to a boxcar integrator connected to a computer. The Faraday rotation ($\Delta\theta$) and the transmission change ($\Delta T/T$) were calculated by the computer. The dual detection technique allowed us to measure both values simultaneously.

3. RESULTS AND DISCUSSION

The probe beam was focused onto a T_0 domain found with the help of Fig. 1. Figures 2 and 3 show the polarization rotation and the transmission change of the probe beam for pump beams at λ_e=1280 and 792 nm, respectively. In panels (a) and (b), the rotation and the transmission change are compared for σ_+ and σ_- polarized pump beams at fixed pump fluence of 33 and 56 GW/cm^2 for λ_e=1280 and 792 nm, respectively. The dependencies of the rotation angle and the transmission change on the pump fluence are plotted in panels (c) and (d).

Independent of the pump wavelength, no rotation was observed before the arrival of the pump beam because of the lack of a net magnetization in AFM NiO. The rotation

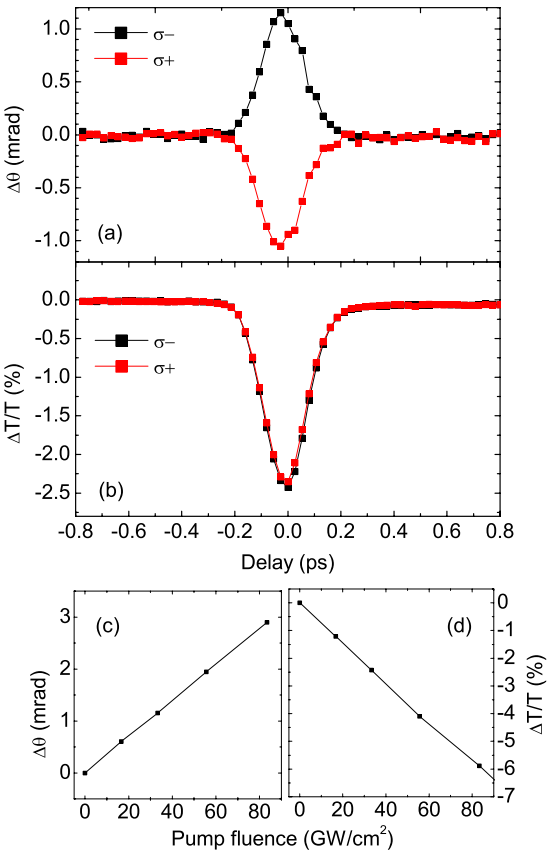

Fig. 2. (Color online) Time-resolved (a) Faraday rotation and (b) transmission change in a NiO (111) sample for pump helicities σ_+ and σ_- with $\lambda_e = 1280$ nm and $\lambda_p = 840$ nm and fixed pump fluence of 33 GW/cm^2. Pump fluence dependence of (c) induced Faraday rotation and (d) transmission change for a σ_- polarized pump beam.

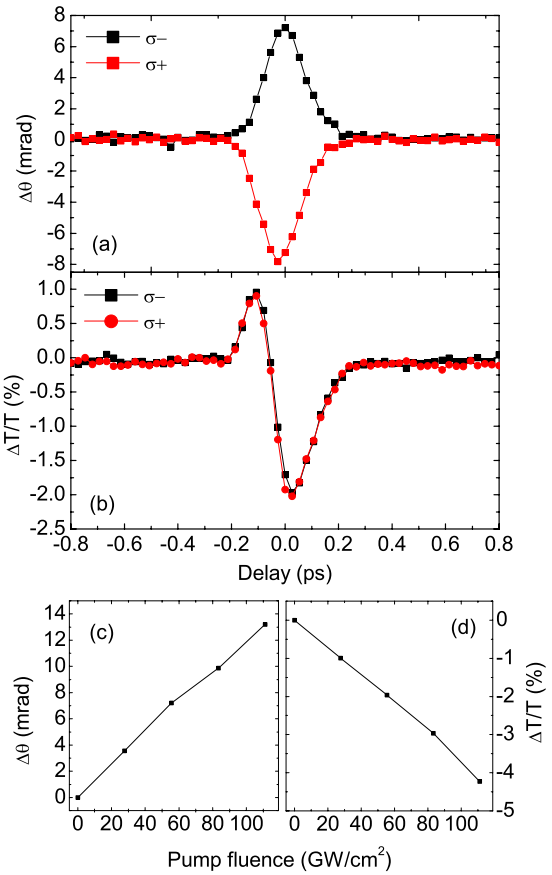

Fig. 3. (Color online) Time-resolved (a) Faraday rotation and (b) transmission change in a NiO (111) sample for pump helicities σ_+ and σ_- with $\lambda_e = 792$ nm and $\lambda_p = 840$ nm and fixed pump fluence of 56 GW/cm^2. Pump fluence dependence of (c) induced Faraday rotation and (d) transmission change for a σ_- polarized pump beam.

was significant when the pump and the probe beams overlapped temporally. The full width at half-maximum of the signal was about 200 fs, which reflects the duration of the chirped WLC probe pulse. The reversal of the rotation angle with the helicity of the pump light is obvious from Figs. 2(a) and 3(a), whereas the transmission change in Figs. 2(b) and 3(b) was not affected by the reversal. In Figs. 2(c) and 3(c), the linear dependence of the rotation angle on the pump laser fluence is consistent with Eq. (4). Yet, the rotation did not depend on the direction of polarization of the probe beam as expected. In summary, our observations clearly indicate that the observed rotation of the linear polarization of the probe pulse was caused by the IFE due to a transient magnetization induced by the circularly polarized pump pulse. The real part of $(-\chi^{(3)}_{xyxy} + \chi^{(3)}_{xyyx})$ at 792 nm pumping is estimated as 2×10^{-21} m^2/V^2 from Eq. (4).

In contrast to the rotation, the transmission change showed a distinct dependence on the pump wavelength. On one hand, Fig. 2(b) reveals a dip of 2.5% around the zero-position of the pump-probe delay. It is ascribed to two-photon absorption [9,17,18], a third-order nonlinear optical effect accompanying the IFE. Linear scaling of the dip amplitude with the pump laser fluence confirms this assumption. On the other hand, Fig. 3(b) shows positive and negative changes around the zero-delay position. The transient increase in transmission cannot be explained by two-photon absorption only. Instead it points to cross-phase modulation [19] as just another third-order nonlinear optical effect. Cross-phase modulation is a phase modulation of a probe pulse due to the change in the refractive index induced by the pump pulse. This leads to a modulation of the spectrum of the weak WLC probe pulse, which is observed as modulation (including an increase) of the transmission in the spectral interval passed through the bandpass filter. Note that the third-order nonlinearity is again confirmed by the linear dependence of the signal on the pump pulse intensity in Fig. 3(d).

An essential feature of all the third-order nonlinear optical effects in Figs. 2 and 3 is that they originate in non-thermal excitation processes. In particular, this holds for the ultrafast magnetization induced transiently via the IFE. The non-thermal nature of the excitation is directly related to the virtual character of the optical excitation. It is evidenced by the absence of residual optical effects in the transmission once the pump beam has passed the sample [9].

Here, the present experiment contrasts with, for example, the generation of spin-polarized electrons by circularly polarized light pulses in semiconductor quantum wells [20]. The latter experiment is based on resonant pumping of an electronic transition with transfer of angu-

lar momentum by the charge carriers. Because of this population, the pump pulse entails a long-lived change in the optical transmission.

What is the mechanism explaining the emergence of a magnetization from virtual optical excitations? In the ground state ($^3\Gamma_2$) of the $Ni^{2+}(3d^8)$ ion, the orbital momentum is quenched due to the orbital non-degeneracy. In the virtually excited state, the orbital momentum is ± 1 depending on the helicity of the pump beam which is coupled to the transient magnetization manifesting as an IFE. Although clarification of the microscopic mechanism of this coupling is beyond the scope of this paper, we point out that both spin and orbital momenta play a role via the spin-orbit coupling. For example, a direct transfer of photon angular momentum to the medium or photo-enhanced transfer between orbital and spin momenta may be involved [7,8,21–24]. Spin-related magnetization was demonstrated by the fact that the induced magnetization at $t=0$ was followed by long-lasting spin oscillations with AFM resonance frequencies [25].

4. SUMMARY

In summary, a variety of transient third-order nonlinear optical effects were observed in antiferromagnetic (AFM) NiO upon illumination with an intense circularly polarized pump pulse and a linearly polarized probe pulse. Aside from cross-phase modulation and two-photon absorption, a rotation of the linear polarization of the probe light was obtained. The rotation was interpreted as an inverse Faraday effect (IFE) caused by the transient nonthermal induction of a magnetization by the pump pulse. It was explained by the coupling between the helicity of the pump pulse and the spin momentum of virtually excited states of the $Ni^{2+}(3d^8)$ ion via the spin-orbit coupling.

ACKNOWLEDGMENTS

This work is supported by KAKENHI (19860020 and (20760008) and by the SPP 1133 of the Deutsche Forschungsgemeinschaft (DFG).

REFERENCES

1. Y. R. Shen, *The Principles of Nonlinear Optics* (Wiley, 1984).
2. K. Kubota, "Two-photon spectroscopy in Faraday configuration. I," J. Phys. Soc. Jpn. **29**, 986–997 (1970).
3. G. Ju, A. Vertikov, A. V. Nurmikko, C. Canady, G. Xiao, R. F. C. Farrow, and A. Cebollada, "Ultrafast nonequilibrium spin dynamics in a ferromagnetic thin film," Phys. Rev. B **57**, R700–R703 (1998).
4. P. J. Bennett, V. Albanis, Y. P. Svirko, and N. I. Zheludev, "Femtosecond cubic optical nonlinearity of thin nickel films," Opt. Lett. **24**, 1373–1375 (1999).
5. R. Wilks, N. D. Hughes, and R. J. Hicken, "Investigation of transient linear and circular birefringence in metallic thin films," J. Phys. Condens. Matter **15**, 5129–5143 (2003).
6. A. V. Kimel, A. Kirilyuk, P. A. Usachev, R. V. Pisarev, A. M. Balbashov, and Th. Rasing, "Ultrafast non-thermal control of magnetization by instantaneous photomagnetic pulses," Nature **435**, 655–657 (2005).
7. F. Hansteen, A. V. Kimel, A. Kirilyuk, and Th. Rasing, "Nonthermal ultrafast optical control of the magnetization in garnet films," Phys. Rev. B **73**, 014421 (2006).
8. F. Dalla Longa, J. T. Kohlhepp, W. J. M. de Jonge, and B. Koopmans, "Influence of photon angular momentum on ultrafast demagnetization in nickel," Phys. Rev. B **75**, 224431 (2007).
9. T. Ogasawara, M. Ashida, N. Motoyama, H. Eisaki, S. Uchida, Y. Tokura, H. Ghosh, A. Shukla, S. Mazumdar, and M. Kuwata-Gonokami, "Ultrafast optical nonlinearity in the quasi-one-dimensional Mott insulator Sr_2CuO_3," Phys. Rev. Lett. **85**, 2204–2207 (2000).
10. P. Borisov, A. Hochstrat, X. Chen, W. Kleemann, and C. Binek, "Magnetoelectric switching of exchange bias," Phys. Rev. Lett. **94**, 117203 (2005).
11. G. Lefkidis and W. Hübner, "First-principles study of ultrafast magneto-optical switching in NiO," Phys. Rev. B **76**, 014418 (2007).
12. A. K. Zvezdin and V. A. Kotov, *Modern Magnetooptics and Magnetooptical Materials* (Taylor & Francis, 1997).
13. W. L. Roth, "Neutron and optical studies of domains in NiO," J. Appl. Phys. **31**, 2000–2011 (1960).
14. I. Sänger, V. V. Pavlov, M. Bayer, and M. Fiebig, "Distribution of antiferromagnetic spin and twin domains in NiO," Phys. Rev. B **74**, 144401 (2006).
15. S. R. Woodford, A. Bringer, and S. Blügel, "Interpreting magnetization from Faraday rotation in birefringent magnetic media," J. Appl. Phys. **101**, 053912 (2007).
16. M. Fiebig, D. Fröhlich, Th. Lottermoser, V. V. Pavlov, R. V. Pisarev, and H.-J Weber, "Second harmonic generation in the centrosymmetric antiferromagnet NiO," Phys. Rev. Lett. **87**, 137202 (2001).
17. S. I. Shablaev and R. V. Pisarev, "Giant nonlinear absorption in the NiO antiferromagnet," Phys. Solid State **45**, 1742–1745 (2003).
18. L. A. Gómez, C. B. de Araújo, L. M. Rossi, S. H. Masunaga, and R. F. Jardim, "Third-order nonlinearity of nickel oxide nanoparticles in toluene," Opt. Lett. **32**, 1435–1437 (2007).
19. K. Ekvall, P. van der Meulen, C. Dhollande, L.-E. Berg, S. Pommeret, R. Naskrecki, and J.-C. Mialocq, "Cross phase modulation artifact in liquid phase transient absorption spectroscopy," J. Appl. Phys. **87**, 2340–2352 (2000).
20. A. Tackeuchi, S. Muto, T. Inata, and T. Fujii, "Direct observation of picosecond spin relaxation of excitons in GaAs/AlGaAs quantum wells using spin dependent optical nonlinearity," Appl. Phys. Lett. **56**, 2213–2215 (1990).
21. V. V. Pavlov, R. V. Pisarev, V. N. Gridnev, E. A. Zhukov, D. R. Yakovlev, and M. Bayer, "Ultrafast optical pumping of spin and orbital polarizations in the antiferromagnetic Mott insulators R_2CuO_4," Phys. Rev. Lett. **98**, 047403 (2007).
22. M. I. Kurkin, N. B. Bakulina, and R. V. Pisarev, "Transient inverse Faraday effect and ultrafast optical switching of magnetization," Phys. Rev. B **78**, 134430 (2008).
23. G. P. Zhang and T. F. George, "Total angular momentum conservation in laser-induced femtosecond magnetism," Phys. Rev. B **78**, 052407 (2008).
24. M. S. Si and G. P. Zhang, "Resolving photon-shortage mystery in femtosecond magnetism," J. Phys. Condens. Matter **22**, 076005 (2010).
25. T. Satoh, S.-J. Cho, R. Iida, T. Shimura, K. Kuroda, H. Ueda, Y. Ueda, B. A. Ivanov, F. Nori, and M. Fiebig, "Spin oscillations in antiferromagnetic NiO triggered by circularly polarized light," arXiv:1003.0820.